Manipulation of the Vacuum to Control Its Field-Induced Decay

Q. Z. Lv, Q. Su, and R. Grobe

Phys. Rev. Lett. **121**, 183606 — Published 2 November 2018
DOI: 10.1103/PhysRevLett.121.183606

Manipulation of the vacuum to control its field-induced decay

Q.Z. Lv[1,2], Q. Su[2,3] and R. Grobe[3]

(1) Max-Planck-Institut für Kernphysik, Saupfercheckweg 1, 69117 Heidelberg, Germany

(2) Beijing National Laboratory for Condensed Matter Physics, Institute of Physics
Chinese Academy of Sciences, Beijing 100190, China

(3) Intense Laser Physics Theory Unit and Department of Physics
Illinois State University, Normal, IL 61790-4560, USA

It has long been predicted that permanent electron-positron pairs can be created from the quantum vacuum at those spatial regions, where an external electric field exceeds a supercritical value. By solving the Dirac equation numerically, we show that the yield of the created positrons at targeted energies can be controlled via a second (sub-critical) electric field that is placed *far outside* the creation zone. This is a first indication of the non-local character of the pair creation process as the second field can be placed at distant spatial regions that are never visited by the created positrons. This rather counter-intuitive phenomenon can be understood in terms of a dressing of the vacuum state long before the particles are actually created. We present an analytical expression for the spectrum of the created particles that describes all quantitative features of this dressing and predicts how the second field can be used to increase as well as decrease the electron-positron yield for desired energies.

7/26/18

The quantum field theoretical vacuum state plays a fascinating role in quantum electrodynamics. For example, it can lead to various unconventional phenomena such as the Casimir force [1], the creation of permanent electron-positron pairs [2], or the occurrence of light-light scattering [3]. A new way to probe its nonlinear properties has become possible due to dramatic advances in laser technology [4,5], which have also motivated numerous theoretical studies with the goal to provide guidance on optimal laser field configurations to maximize the observed particle yield [6]. Each of these studies focused on how the *local* properties of the external radiative environment *inside* the pair creation zone can be exploited to control the pair-creation yield, leading in some cases to unexpected predictions.

For example, in the limit of an infinitely extended electric field, the Schwinger expression [7] predicts a monotonic increase of the pair creation rate with increasing field strength, which needs to be revised for the non-local nature of the process in spatially inhomogeneous field configurations [8]. A recent work [9] has suggested that the particles are not necessarily created in those spatial regions of the interaction zone where the electric force field is largest. In fact, for some electromagnetic field configurations, particles cannot even be created in those regions where the field is largest.

In this Letter, we report on yet another counter-intuitive phenomenon that illustrates the non-local nature of the pair-creation process. It turns out that the energy spectra of the created particles can be manipulated by a second (and much weaker) external field that is localized far outside the pair creation zone. Even more surprisingly, the energy distribution of the positrons can still be strongly affected, even if this second field is placed at a spatial region, that is never visited by the created positrons.

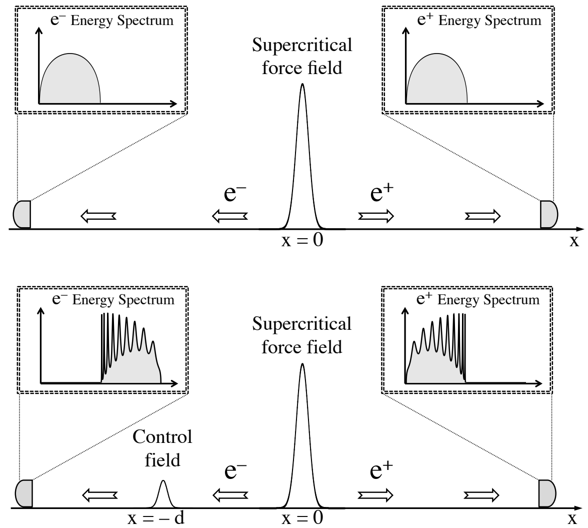

Figure 1 Sketch of the electric field configuration based solely on a supercritical field at x=0 (top panel). In the bottom panel a second (control) field at x=–d is added. Electron-positron pairs are created from the vacuum solely by the supercritical field and the particles' energy is detected. Positrons are ejected to the right and therefore cannot interact directly with the control field.

Before we discuss this new effect more quantitatively, let us illustrate first in the two panels in Figure 1 the basic geometry of the one and two-field configurations. The top panel shows a typical one-field set-up for the usual electron-positron pair creation process. Here we assume for simplicity that the static and localized electric field is placed at x=0 and symmetric under spatial inversion. Its strength is assumed to be supercritical, i.e. its associated potential energy V_S for a positron exceeds $2mc^2$, such that after its turn on, it generates a steady flux of electron-positron pairs. We assume that this field is oriented such that the created electrons (positrons) are accelerated to the left (right). In order to measure the energy distribution of the created particles, two detectors are placed far away from the interaction zone. As the field is chosen symmetric, the energy spectra of both particles are identical, as sketched in the top panel.

In the bottom panel, we have repeated the identical configuration, however, now a second (non-supercritical) field has been placed at x= – d. As this control field is located *far outside* the creation zone, the created positrons cannot visit this spatial region and, based on locality, one could expect that the presence of this field cannot affect the dynamics of the created positrons. The positronic spectrum should therefore be identical to the one obtained from the one-field configuration. It is the main purpose of this Letter to demonstrate that the pair-creation process has unexpected non-local features with regard to the particles. In fact, we will provide numerical as well as analytical evidence that the spectra of both particle species depend crucially on the control field. This finding also suggests a novel means of manipulating the pair creation process from outside the pair creation zone.

In order to describe this new phenomenon more quantitatively, we have to briefly summarize the theoretical framework that permits us to compute the energy spectra, pair creation rates and spatial distributions of the particles. Below we will also present analytical expressions for the energy spectra. In computational quantum field theory the interaction of the vacuum with static electromagnetic fields is often modelled by the Hamiltonian $H = c\, \boldsymbol{\alpha}\, \mathbf{p} + mc^2 \beta + V(\mathbf{r})$, which governs both the time evolution of the four spinor components of the electron-positron quantum field operator (via the Dirac equation) and the dynamics of the fermion's creation and annihilation operators (via the Heisenberg equation). Here $\boldsymbol{\alpha} \equiv (\alpha_1, \alpha_2, \alpha_3)$ and β denote the set of the four 4×4 Dirac matrices and $V(\mathbf{r})$ is the potential energy of a positron in the electric field.

The quantum field operator $\Psi(x,t)$ can be expanded into eigenstates of the force-free Hamiltonian with positive and negative energies, i.e., $H_0 |p;u\rangle = E|p;u\rangle$ and $H_0 |p;d\rangle = - E|p;d\rangle$, where $E(p) \equiv [m^2c^4+c^2p^2]^{1/2}$, leading to $\Psi(x,t) \equiv \Sigma_p [\, b(p,t)\, |p;u\rangle + d(p,t)^\dagger\, |p;d\rangle]$, where the operators fulfill $[b(p),b(k)^\dagger]_+ = [d(p),d(k)^\dagger]_+ = \delta_{p,k}$ and $[b(p),b(k)]_+ = [d(p)^\dagger,d(k)^\dagger]_+ = [b(p),d(k)^\dagger]_- =0$.

The momentum (and energy) spectra of the created fermions can be computed via the expectation values of the positronic and electronic creation and annihilation operators as $N^{(+)}(p,t) \equiv \langle b(p,t)^\dagger b(p,t)\rangle$ and $N^{(-)}(p,t) \equiv \langle d(p,t)^\dagger d(p,t)\rangle$. We can define the energy spectra as $N^{(\pm)}(E,t) \equiv N^{(\pm)}(p,t)\, dp/dE$, such that we have consistently for the total number of created pairs, $N(t) = \int dE\, N^{(\pm)}(E,t)$. Introducing the transition matrix elements $U_{p,k}(t) \equiv \langle p;u|U(t)|k;d\rangle$, where $U(t)$ is the time-ordered evolution operator associated with the Hamiltonian H, we obtain

$$N^{(+)}(p,t) \equiv \langle b(p,t)^\dagger b(p,t)\rangle = \Sigma_k |U_{p,k}(t)|^2 \tag{1a}$$

$$N^{(-)}(p,t) \equiv \langle d(p,t)^\dagger d(p,t)\rangle = \Sigma_k |U_{k,p}(t)|^2 \tag{1b}$$

The two energy densities can be significantly different for some electromagnetic field configurations, such as the one shown in the bottom panel of Fig. 1.

Due to the orientation of the electric fields, we describe the dynamics here by a Hamiltonian in which the fields are coupled to a positive charge, such that the two expressions (1a and b) have the obvious interpretation that is consistent with Dirac's hole theory based on positrons. Here the depletion of the initially occupied negative energy state $|p;d\rangle$ (as a member of the Dirac sea that represents the vacuum) into the states $|k;u\rangle$ corresponds to the creation of an electron with energy E(p), while the transition to the upper state $|p;u\rangle$ (from *all* lower states) describes the creation of a positron with energy E(p). Equivalently, for consistency, the prediction could be obtained from the corresponding charge-conjugated (and more traditional) hole theory, in which the initial Dirac state $|p;d\rangle$ is evolved under the electronic Hamiltonian, such that here the depletion of the state $|p;d\rangle$ to all states $|k;u\rangle$ corresponds to the creation of a positron with energy E(p).

Let us discuss next the numerical data that were obtained. The two electric fields were modeled by the two-step potential energy $V(x) = V_c\,[1-\mathrm{Tanh}((x+d)/w)]/2 + V_S\,[1-\mathrm{Tanh}(x/w)]/2$, such that $V(x = -\infty) = V_c + V_S$ and $V(x = \infty) = 0$. The spatial extension of both fields is w. The energy spectra depend qualitatively on time and reflect the various stages of the particle creation. For short times, the spectra decrease monotonically with increasing energy E. We focus here on the long-time regime, which is independent of the turn-on pulse shape. Here the total number of particles N(t) grows linearly as a function of time $N(t) = \Gamma\, t$, and Γ is the vacuum's decay rate. As the number density at each energy, $N^{(\pm)}(E,t)$, grows linearly in time, for better visibility we have renormalized the spectra and graphed the curves $N^{(-)}(E,t)\,(2\pi/t)$ and $N^{(+)}(E,t)\,(2\pi/t)$ in Figure 2. For comparison, we denote by the dashed lines the corresponding spectra for the case where the control field is absent (top panel of Figure 1).

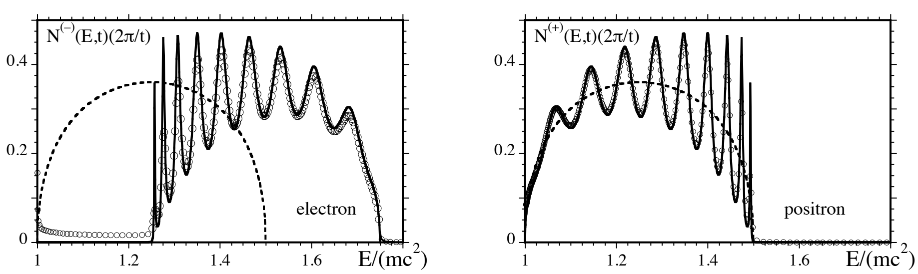

Figure 2 The (renormalized) energy spectra $N(E,t)\,(2\pi/t)$ of the created electrons (left) and positrons (right). For comparison, the dashed lines are the corresponding spectra without the second field. The open circles denote the numerical data obtained from the simulation, while the solid line is the analytical expressions according to Eq. (2). The potential energy is given by $V(x) = V_c[1\text{-}\mathrm{Tanh}((x+d)/w)]/2 + V_S[1\text{-}\mathrm{Tanh}(x/w)]/2$, where $V_S = 2.5mc^2$, $V_c = 0.25mc^2$, $w=0.075\ \hbar/(\alpha mc)$ and $d=0.2\ \hbar/(\alpha mc)$, the interaction time was $t=0.045\ \hbar/(\alpha^2 mc^2)$, and α is the fine structure constant.

In the absence of the control field (V_c=0), the electronic and positronic spectra (dashed lines) are identical at any time, due to the assumed spatial symmetry of the supercritical field, i.e. $V'(x) = V'(-x)$. The spectrum of the electrons is modified by V_c in two ways. First, the fact that it is shifted to higher energies (by the amount V_c) is expected, as, in contrast to the positrons, the electrons actually do pass through the region of the control field (at $x = -d$) and therefore experience an acceleration to higher energies before their detection. We also note that the control field superimposes an oscillatory structure, where higher frequency oscillations are observed at the lower energetic part of the spectrum.

Remarkably, the positronic spectra with and without the control field are also entirely different. While for both field configurations the observed range in energy (from $E=mc^2$ to $E=mc^2-V_S$) is identical, the presence of the control field leads to strong oscillatory modulations of the spectrum [10], whose amplitude is comparable to the overall strength of the signal. In contrast to the electronic spectra, here the frequency of these oscillations increases with higher energies. It is important to note that the maxima in the spectra are *higher* than the spectrum in the absence of the control field (dashed line). In other words, the control field can be used to *enhance* the creation of positrons for specific energies. In our opinion, the observed amplification also rejects a possible explanation of this phenomena that is based on the assumption that created electrons could be reflected by the control field, return to the creation zone and then subsequently interfere with the creation process at x=0. This process is not so important here, as the fermionic Pauli suppression mechanism usually decreases the creation rate [11] at any energy. In addition, the reflection likelihood of electron decreases rapidly with increasing V_c, while, as we show below, that the oscillation amplitudes actually increase.

The computational approach permits us also to examine the pair creation dynamics from a spatially resolved perspective. We show in Figure 3 the corresponding spatial densities of the created electrons and positrons. As expected, the supercritical field ejects the electrons (positrons) to the left (right). The increased density inside the creation zone should not be overinterpreted, as the computation of the density was based on the projection of the electron-positron field operator on field-free energy eigenstates, which are not so meaningful in those regions where the electric field is supercritical. While the electric current density can be computed unambiguously everywhere in space, it is presently not fully understood how one can even distinguish within the interaction zone between positively and negatively charged particles.

The decrease of the density for x<–d reflects the higher speed of the electrons in this domain compared to x>-d, i.e., there are less particles per unit length.

The key observation here is that the positronic density (dashed line) vanishes indeed entirely for x<0 and particularly close to x=–d, where the control field is located. This clearly shows that the positrons cannot interact with the control field after their creation.

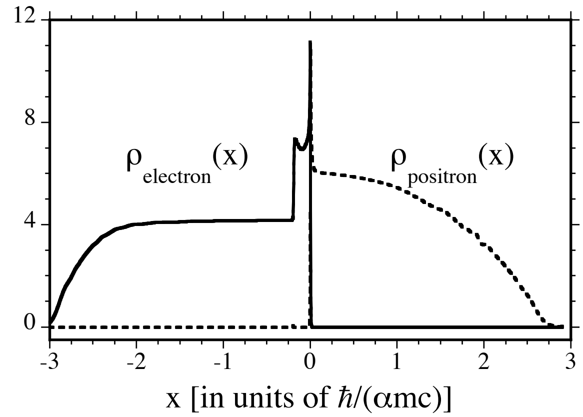

Figure 3 The spatial probability density of the created electrons (continous line) and positrons (dashed line) after time t=0.024 $\hbar/(\alpha^2 mc^2)$. Other parameters are identical as in Fig. 2.

After the presentation of the numerical data, we provide an intuitive explanation of this non-local behavior, which is suggested by the mathematical structure of the Dirac sea picture. As mentioned above, here the vacuum state is represented by fully occupied negative-energy eigenstates of the free Dirac Hamiltonian. The initial population of these states acts as an infinite reservoir for the creation of particles, associated with the transition to the Hilbert space spanned by positive energy eigenstates. In contrast to the state of the created positrons, these states are infinitely extended in space and therefore their dynamics is impacted not only by the supercritical but also by the control field. These two fields permit therefore constructive as well as destructive interferences, depending on the wavelength of the Dirac sea state. As the two fields are chosen time-independent, a final positronic state with (positive) energy E can be traced back uniquely to the decay of a single Dirac sea state [12] with a (force-free) negative energy given by $E–V_c–V_s$ that moves to the right (with a negative momentum). The fact that a state with negative momentum has nevertheless a positive probability current density is characteristic of all negative energy states. In addition, the removal of population of the same state corresponds also to the creation of an electron with positive energy $|E–V_c–V_s|$.

The higher frequency of the energy modulation for large positronic energies E can also be easily understood, as the corresponding Dirac sea state takes the momentum $k \equiv – [(V_s–E)^2 –$

$m^2c^4]^{1/2}/c$ between $x{=}{-}d$ and $x{=}0$. The subset of resonant momenta therefore has to fulfill $|k_n|\, d = n\hbar\pi$, with n=1,2, …, leading to an amplification for energies $E_n = V_s - [m^2c^4 + (n\hbar\pi/d)^2\, c^2]^{1/2}$. As the largest possible momentum $|k|$ (associated with the lowest positron energy $E = mc^2$) is $|k| \equiv [(V_s - mc^2)^2 - m^2c^4]^{1/2}/c$, therefore, the total number of maxima is given by the integer part of $d[(V_s - mc^2)^2 - m^2c^4]^{1/2}/(c\hbar\pi)$, which amounts for our parameters to $n_{max}{=}9$, which is in full agreement with the number of peaks shown in Fig. 2. The same argument predicts the occurrence of the higher frequency oscillations at the lower energetic part of the spectrum for the electrons with energy $|V_c+V_s-E|$.

Finally, we will use this understanding of the vacuum's dressing effect to provide a quantitative model that can reproduce all key features of the spectrum. As detailed in a prior work [11-14], the energy dependence of the electrons as well as positrons can be related to the quantum mechanical transmission coefficient of an incoming wave packet. If we assume that the spatial widths of the two electric fields at $x{=}{-}d$ and $x{=}0$ are both infinitely narrow, then this coefficient can be obtained from the stationary energy eigenstates of the corresponding two-step potential. For reasons of brevity we state here the final answer for $mc^2 < E < mc^2 - V_s$.

$$N^{(+)}(E,t) = t/(2\pi\hbar)\, 2c^2\, p\, q\, /[2m^2c^2\, V_c\, V_s\, \mathrm{Sin}^2(k\, d/\hbar)/\, k^2 + E(V_s+V_c-E) + 2c^2\, p\, q + m^2c^4] \qquad (2)$$

where $p \equiv [E^2 - m^2c^4]^{1/2}/c$, $q \equiv [(V_s+V_c-E)^2 - m^2c^4]^{1/2}/c$ and $k \equiv [(V_s-E)^2 - m^2c^4]^{1/2}/c$.

The corresponding spectrum of the created electrons $N^{(-)}(E,t)$ is different in two respects. First, the more frequent oscillations occur on the lower energy side, so its spectrum is reversed with regard to the central energy $E = V_s/2$. In addition, in contrast to the positrons, it is also shifted, as the escaping electrons pass through the second field at $x = -d$, which gives the electrons an additional energy boost by the amount of V_c. Therefore, the positronic and electronic energy spectra are related for long times via $N^{(-)}(E,t) = N^{(+)}(V_c+V_s - E,t)$, where $mc^2+V_c < E < V_c+V_s - mc^2$. For comparison, we have graphed the predictions of the two analytical expressions by the continuous lines in Figure 2. The agreement with the exact numerical spectra (open circles) for the finite time $t{=}0.045\ \hbar/(\alpha^2mc^2)$ and the electric fields with non-zero extension is excellent. The only difference is associated with the fact that the analytical expression describes the true spectrum only for infinitely long times, whereas the numerical spectrum also describes particles that were created at the early time stages before the steady state was established.

The availability of a fully analytical pair creation rate permits us to address two important questions with regard to the scaling of this phenomenon. In our opinion, the most important conclusion is the fact that the amplitudes of the oscillations do *not* depend on the distance d between the two fields. This means that this field can be placed arbitrarily far away from the interaction zone in this particular one-dimensional configuration and can still affect the positrons with equal strength. However, a large d also leads to very narrow oscillations that could be hard to be resolved in the spectrum. Second, while the location and the strength of the control field V_c can be specifically tailored to increase the created particles at any desired energy, the total vacuum decay rate (the energy integral over the renormalized spectrum) cannot be increased by V_c and always decreases with increasing strength V_c, as some portion of the right traveling Dirac sea states are (unavoidably) reflected at $x=-d$ and therefore cannot contribute to the pair creation process at $x=0$.

The interpretation of the vacuum's dressing phenomenon can be further illuminated if we examine the effect of a different alignment of the control field on the positrons' spectrum. This comparison can be achieved by reversing the sign of V_c in Eq. (2). An opposite orientation (V_c negative) manifests itself in three different ways. First, the energy range of the detected positrons is now reduced by $|V_c|$ due to the fact that only those Dirac sea states with sufficiently large energy can overcome the energy "barrier" provided by an electric control field that now points to the left. This observation is an alternative manifestation of the non-locality. By "cutting off" certain Dirac sea states from reaching the supercritical field, the pair creation process can be inhibited for positrons with a desired energy. Second, the energies for maxima and minima in the spectrum are exchanged, as the resonance condition and the resulting phase relationships are shifted by π under the sign change of V_c. Third, the envelope curve that describes the energy dependence of the amplitudes for each maximum takes a different form. This envelope can be obtained by setting the term $2m^2c^2\, V_c\, V_s\, \mathrm{Sin}^2(k\, d/\hbar)/\, k^2$ in Eq. (2) to zero leading to max $[N^{(+)}(E,t)] = t/(2\pi\hbar)2c^2pq/[E(V_s+V_c-E)+2c^2pq+m^2c^4]$. For larger energies $E>V_s/2$ this envelope increases for $V_c>0$ (as shown in Fig. 2), while for $V_c<0$, it would decrease.

In summary, the main purpose of this work is to provide a first proof of principle that, while the pair creation process creates entangled particles, it is not necessarily local (from the perspective of the created particles) and therefore can be manipulated via suitable external control fields that are placed far outside the creation zone, even at regions that are never visited by the created positrons. The manipulation of the vacuum modes is not a new phenomenon in itself, for example, it was demonstrated that the spontaneous emission rate of atoms can be inhibited or enhanced [15] by placing the atom in a cavity [16].

For conceptual simplicity, our phenomenon was illustrated for a spatially confined geometry. In order to show that the effects can be in principle measured experimentally, we have examined numerically a situation where 30KeV x-ray lasers [19] were modeled by inhomogeneous external fields. The tightly focused radius was of the order of 0.1 nm while the distance between the two fields can be several nanometers. In this setup, a stationary creation rate, which can be two times larger for some specific energies due to the control field, is established after several femtoseconds. For practical reasons, a high frequency laser is recommended in this setup, while a low frequency laser (for which the analytical model was provided) could be less feasible. On the other hand, the inclusion of the temporal structure of the x-ray field would also trigger pair creation due to multiphoton processes, for which the dressing of the vacuum might be more complicated in realistic laboratory conditions.

Acknowledgements

We would like to thank Profs. N. Christensen, C.H. Keitel and G.H. Rutherford for helpful discussions. QZL would like to thank ILP for the nice hospitality during his visit to Illinois State. This work has been supported by the NSF, the NSFC (#11529402), Research Corporation and the Strategic Priority Research Program of the Chinese Academy of Sciences (Grant No. XDB16010200). QZL acknowledges the support from the German Humboldt Foundation.

References

[1] For recent works on the Casimir effect, see, E.A. Chan, S.A Aljumid, G. Adamo, A. Lliotis, M. Ducloy and D. Wilkowski, Science Adv. 4, 4223 (2018); P. Rodriguez-Lopez, W.J.M. Kort-Kamp, D.A.R. Dalvit and L.M. Woods, Nature Comm. 8, 14699 (2017);

[2] For a reviews, see, e.g., A. Di Piazza, C. Müller, K.Z. Hatsagortsyan and C.H. Keitel, Rev. Mod. Phys. 84, 1177 (2012) and B.S. Xie, Z.L. Li, S. Tang, Matter and Radiation at Extremes 2, 225 (2017).

[3] For example, see B. King, A. Di Piazza, and C. H. Keitel, Nature Photon. 4, 92 (2010) and more recently, J. Ellis, N.E. Mavromatos and T. You, Phys. Rev. Lett. 118, 261802 (2017).

[4] G.A. Mourou, T. Tajima and S.V. Bulanov, Rev. Mod. Phys. 78, 309 (2006).

[5] For recent advances and numerous references, see, e.g. https://eli-laser.eu/

[6] For recent work on optimization see, e.g., C. Kohlfürst, M. Mitter, G. Von Winckel, F. Hebenstreit and R. Alkofer, Phys. Rev. D 88, 045028 (2013); A. Gonoskov, I. Gonoskov, C. Harvey, A. Ilderton, A. Kim, M. Marklund, G. Mourou and A. Sergeev, Phys. Rev. Lett. 111, 060404 (2013). S.S. Dong, M. Chen, Q. Su and R. Grobe, Phys. Rev. A 96, 032120 (2017).

[7] J.S. Schwinger, Phys. Rev. 128, 2425 (1952).

[8] H. Gies and K. Klingmüller, Phys. Rev. D 72, 065001 (2005).

[9] Q.Z. Lv, J. Unger, Y.T. Li, Q. Su and R. Grobe, Euro. Phys. Lett. 116, 40003 (2016).

[10] Oscillatory energy spectra can also occur in pair creation processes triggered by sequences of time-dependent pulses, see, e.g., E. Akkermans and G.V. Dunne, Phys. Rev. Lett. 108, 030401 (2012). However, this interference effect is different from the one discussed in this work.

[11] P. Krekora, Q. Su and R. Grobe, Phys. Rev. Lett. 92, 040406 (2004).

[12] Q.Z. Lv, S. Dong, C. Lisowski, R. Pelphrey, Y.T. Li, Q. Su and R. Grobe, Phys. Rev. A 97, 053416 (2018).

[13] For recent applications, see, Fillion-Gourdeau, E. Lorin and A.D. Bandrauk, Phys. Rev. Lett. 110, 013002 (2013).

[14] F. Hund, Z. Phys. 117, 1 (1941).

[15] P. Goy, J.M. Raimond, M. Gross and S. Haroche, Phys. Rev. Lett. 50, 1903 (1983) and R.G. Hulet, E.S. Hilfer and D. Kleppner, Phys. Rev. Lett. 55, 2137 (1985).

[16] However, here the vacuum is bosonic and the cavity leads to a discrete mode spacing. As a

result, the modification of the decay rate occurs here only after the created light has hit the cavity wall and returned to the atom [17,18], while in our case the resonance condition is established by the occupied negative energy modes, i.e. the vacuum itself.

[17] J. Parker and C.R. Stroud, Jr., Phys. Rev. A 35, 4226 (1987).

[18] H. Gießen, J.D. Berger, G. Mohs and P. Meystre, Phys. Rev. A 53, 2816 (1996).

[19] L. F.DiMauro et al., J. Phys. Conf. Ser. 88, 012058 (2007); M. Altarelli et al., Technical Design Report of the European XFEL, DESY 2006-097 (http://www.xfel.net).